Journal of Coastal Research	10	1	158 169	Fort Lauderdale, Florida	Winter 1994

Development of a Non-linear Porous Media Flow Relationship for Oscillatory Unsteady Flow

Kevin R. Hall†, Greg M. Smith‡ and David J. Turcke†

†Department of Civil Engineering
Queen's University
Kingston, Ontario, Canada

‡Delft Hydraulics Laboratory
Emmeloord, The Netherlands

ABSTRACT

HALL, K.R.; SMITH, G.M., and TURCKE, D.J., 1994. Development of a non-linear porous media flow relationship for oscillatory unsteady flow. *Journal of Coastal Research*, 10(1), 158–169. Fort Lauderdale (Florida), ISSN 0749-0208.

In recent years, numerical modelling of non-stationary porous media flow resulting from wave interaction with granular media in coastal areas (such as wave interaction with breakwaters, flow in the seabed and flow in submerged granular structures) has been the topic of much research. Many models have been based on non-linear porous media flow laws such as the Forchheimer equation which is based on unidirectional, non-linear flow.

This paper presents the results of testing undertaken in an oscillatory water tunnel in which various media were subjected to rapidly varying oscillatory flow, such as that experienced by granular structures subjected to wave action. Results of the experiments are compared with the Forchheimer equation. It was found that the addition of an inertial term would greatly increase the accuracy of the Forchheimer equation. However, problems still exist in predicting the steady and unsteady flow coefficients for most granular media, unless carefully controlled permeameter tests are undertaken. As an alternative, the resistance of the media was formulated directly in terms of the hydraulic properties of the oscillatory flow and the properties of the medium. This new relationship resulted in excellent agreement between experimental and predicted hydraulic gradient.

ADDITIONAL INDEX WORDS: *Porous media flow, breakwaters, wave-structure interaction, unsteady flow, oscillatory flow.*

INTRODUCTION

This paper describes a research programme designed to investigate the effects of temporal inertia on the resistance to rapidly varying oscillatory flow through a porous medium. The physical mechanisms governing the phenomenon of stationary flow have been extensively researched in the past and are well understood. Few experimental studies, however, have examined the effects of accelerated flow. Non-stationary porous media flow occurs in several situations when waves come into contact with a granular medium; flow in the seabed under shallow water waves, flow through rubble foundations under caissons, and flow through breakwaters subjected to wave attack, for instance. For the specific case of wave motion the flow field will be oscillatory so the present study was aimed at investigating the flow resistance of porous media subject to unsteady oscillatory flow.

Granular media in the above-mentioned cases are typically randomly placed particles (rock, gravel, sand, *etc.*) characterized by a grain size distribution curve and uniformity coefficients. The resistance of this material to flow (or its permeability) is dependent upon many parameters such as particle shape, orientation, surface roughness, porosity, *etc.*, most of which cannot be controlled even in a laboratory environment. To eliminate the effects of such random quantities, tests were conducted on uniformly packed spheres of equal diameter. The influence of porosity on the resistance was tested by packing the spheres in dense and loose configurations. The influence of diameter was tested by using two different sizes of spheres, each size tested in both packing arrangements. Finally, one sample of randomly placed stone was tested to see the magnitude of the effects of the random properties of the stones.

The tests were conducted in the oscillating water tunnel at the Coastal Engineering Laboratory, Queen's University. For each material in each of the packing arrangements, eight tests were performed by varying the oscillation periods and amplitudes. This allowed the influence of oscillation period and amplitude, grain size and porosity on the resistance to the flow to be studied. Previ-

92140 received 6 December 1992; accepted in revision 12 July 1993.

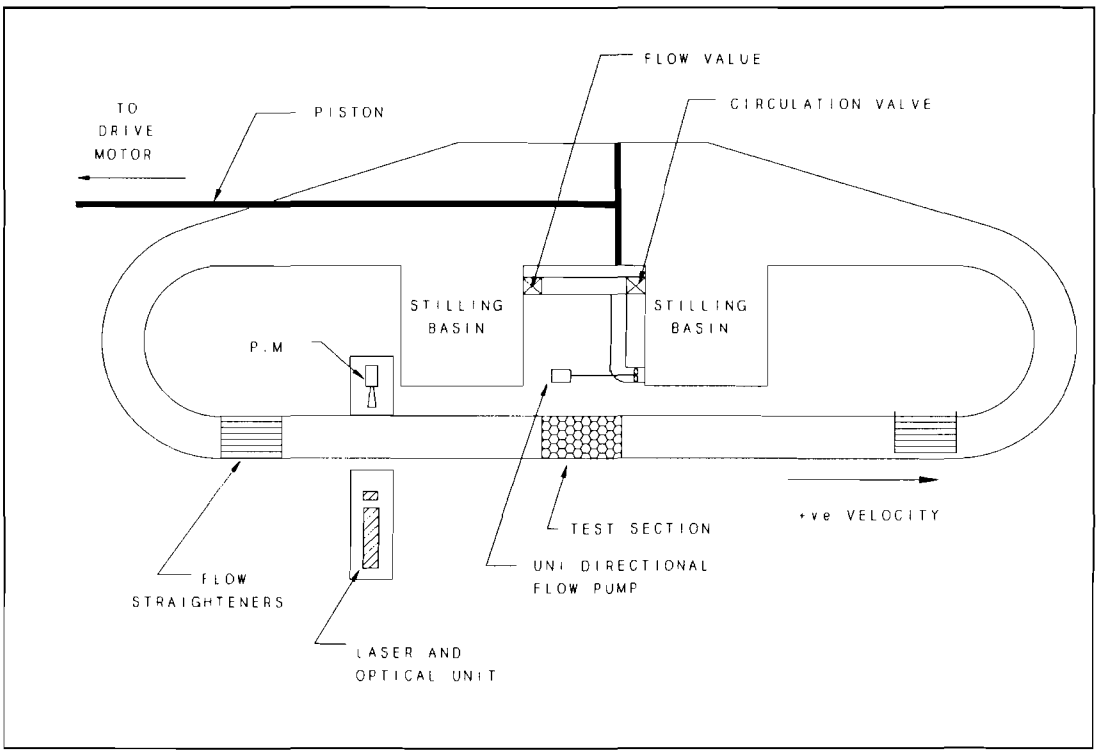

Figure 1. Layout of oscillating water tunnel.

ously, the only way to evaluate the inertial effects for unsteady flow was to assume that the steady-state coefficients in the governing flow equation apply also in unsteady flow (HANNOURA and MCCORQUODALE, 1978; MCCORQUODALE and ABDEL-GAWAD, 1985). The main goal of this study was to check this assumption and to examine the magnitude of the temporal inertial effects.

When the flow is modelled numerically, the effects of the properties just mentioned must be formulated. Numerical models require the definition of the velocity and pressure fields across the medium. Most numerical models use a flow law which describes the energy loss across the medium in terms of the average velocity of the flow. The velocity field within the medium must be computed by applying the equations of momentum and continuity to calculate the velocity using external boundary conditions, usually the pressure field at the boundary of the medium. For the particular case of flow generated by wave motion, it would be helpful to describe the energy loss in terms of the wave characteristics directly, *i.e.* the period and amplitude of oscillation, along with the properties of the medium, so that no velocity calculations need to be made. This will eliminate the need to evaluate unsteady and steady flow coefficients for a given medium. HALL (1987) and HALL and SMITH (1992) have shown that existing formulations for evaluation of the "a" and "b" coefficients in the Forchheimer relationship,

$$i = aq + bq^2, \quad (1)$$

where i = hydraulic gradient and q = bulk or macroscopic velocity are not reliable.

EXPERIMENTAL PROCEDURE

Oscillating Water Tunnel

All experiments were performed in a horizontal oscillating water tunnel (Figure 1). Both oscillatory flow and steady unidirectional flows could be generated by the drive mechanisms. The measuring section in the tunnel had cross sectional dimensions of 1 m by 0.5 m (height by width) and the lengths of the test samples were set equal to

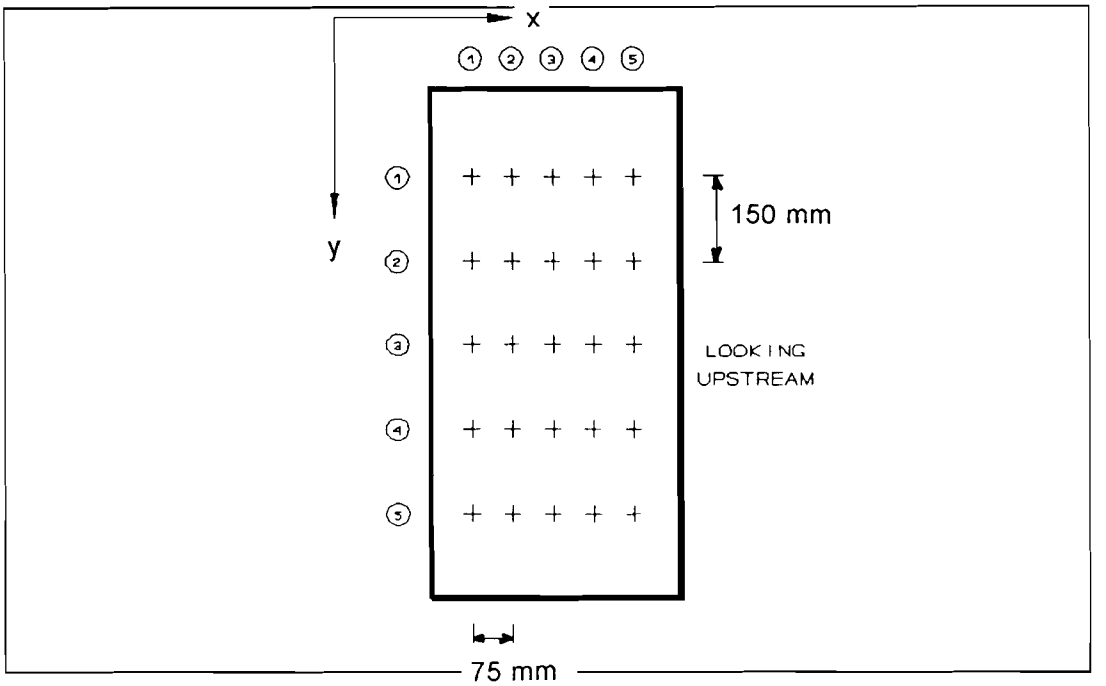

Figure 2. LDA velocity grid.

20 times the characteristic dimension of each material. Test samples were installed in the central portion of the working section and pressure transducers were fitted within the test samples. Test samples were secured using sheets of expanded steel installed at each end of the samples.

The tunnel was filled with water to a head of about 1.5 metres above the top of the working section to ensure that no free surface existed during testing. Steady flows were generated by a constant speed pump located within the central oval of the tunnel. The direction of flow defined as positive is indicated in Figure 3.1. Subsequent references to upstream and downstream of the test section are made with respect to this direction.

Oscillatory flows were generated by a piston driven from a variable speed motor. The piston, located at the rear side of the tunnel between the two stilling basins, measured 2 m by 2 m and could generate large flows in the working section of the tunnel, with the area ratio being 8:1 (piston bore: test section). Both stoke length and oscillation period could be varied. Periods tested ranged from a maximum of 13 seconds to a minimum of 3 seconds. For the oscillatory tests it was important to relate the phases of the velocity and the pressure measurements. For this reason a trigger was installed on the piston arm to ensure that all measurements commenced at the same position within the cycle.

The goal of the study was to relate a bulk or macroscopic velocity flow to the associated pressure response. Some previous researchers determined this velocity by measuring the flow rate and dividing this by the cross sectional flow area (in steady flow tests). A drawback of this method is that a higher flow rate occurs near the edges of the section than through the centre section due to the smooth contact surface of the permeameter. This gives an artificially high value for the bulk velocity; DUDGEON (1964) estimated the velocity determined in this manner to be 10 to 15% higher than the actual velocity in the core of the sample. To prevent this occurrence it was decided to measure velocities directly on a grid in the central portion of the cross section with a Laser Doppler Anemometer (LDA). This instrument has the advantage that point velocity measurements are possible without physical intrusion into the flow channel. The grid is shown in Figure 2. The signal from the laser was sampled via an analogue to

digital convertor on-board a VAX microcomputer. Acquired data was carefully screened and processed with software developed particularly for this application.

For steady flow tests, the velocities were observed to fluctuate about a mean value, depending on the location of measurement. A straight mean value was computed and was used as the representative velocity for the particular point of measurement. After the mean velocities were computed for each point of measurement, the velocity distribution in the cross section was determined. The bulk flow rate was computed by taking the average of all point velocities. Mean values of velocity for the points within the central core of the tunnel yielded a similar value as the average of all points. Consequently the average of all data was considered representative of the mean bulk flow rate.

For the oscillatory flow tests, velocity readings taken at different locations throughout the measurement cross section were spatially averaged to obtain one average velocity record for the flow test. The averaging procedure reduced any non-uniformities in the velocity record. Finally, this spatial average velocity record for each test was phase averaged to reduce small irregularities in the record as well as the space required to store the data.

Pressures inside the sample were recorded with 0 to 40 kPa (0–6 psi) Data Instrument AB pressure transducers and a Pacific 16 channel amplifier linked via an analogue to digital converter to a microcomputer. Sampling commenced upon activation of the trigger described earlier so pressure measurements could be made simultaneously with the velocity readings. Pressure readings were sampled for 60 seconds at 10 Hz for all tests.

Four transducers were used for each test; two located at each end of the sample along the centre line, inset 3 diameters from the face of the sample as recommended by WRIGHT (1968). For the first test series (75 mm spheres, rhombohedral packing) both transducers at each end were installed side by side at mid height but facing opposite directions. This tested the repeatability of measurements and the effect of orientation. Readings from each pair were identical. For subsequent test series the transducers at each end were spaced apart vertically by about one-third of the height of the sample, and were installed along the centre line of the section. This enabled a determination of any vertical pressure variations in the sample. For the tests with spheres, the transducers were mounted inside the spheres with their diaphragms flush with the sphere surface, enabling measurement without obstructing the flow. For the rock sample, the transducers were installed into voids and held in place by rocks placed around them. The diaphragms were protected by a brass screen fastened to the transducer.

Test Materials

Tests were conducted on three different materials: 75 mm diameter spheres, 42 mm diameter spheres and one sample of large uniformly graded rock (M_{50} = 1.4 kg). The equivalent D_{50} of the rock was 100 mm, which is the diameter of a sphere with equal mass (M_{50}) and with a relative density of 2.65.

Each type of sphere was tested in simple cubic and rhombohedral packing arrangements, corresponding to maximum and minimum porosity values that can be achieved using spheres. For the 75 mm spheres, the diameter, D, is relatively large compared to the size of the tunnel (D_T), exceeding the maximum value of $D/D_T = 0.1$ recommended by ROSE and RIZK (1948) in order to minimize wall effect. However, this value has not conclusively been proven to be absolute. More recent work into the nature of wall effect (DYBBS and EDWARDS, 1982; WRIGHT, 1968) has suggested that the effect is significant only within 2 or 3 grain diameters of the wall. The smaller spheres had a D/D_T ratio of 0.1.

It must be noted here that rhombohedral packing is not symmetrical in three dimensions. In two dimensions straight and narrow channels pass through the sample but in the third dimension no such channels exist. Thus permeability is direction dependent for a given porosity. Both samples tested in the present study were installed so that the straight flow channels were not aligned with the direction of flow; this represented the minimum attainable permeability offering the maximum resistance (*i.e.* maximum tortuosity).

Porosity

Almost all previous studies into porous media flow have used the sample porosity as a fundamental variable governing the flow. Typically, the porosity, n, is of primary importance in parameterization of the Forchheimer coefficients as they have been found to vary as a function of n^{-1} to n^{-6}. This is very unfortunate because accurate measurement of the porosity is most difficult to achieve and is usually associated with the largest

errors. DUDGEON (1968) pointed out that it is impractical to spend much effort in making highly accurate velocity and pressure measurements because the errors in porosity determination greatly outweigh those errors associated with velocity and pressure measurements.

Difficulties in measuring the porosity arise primarily from the fact that a certain amount of water adheres to the surfaces of the particles in the sample and air bubbles become trapped between particles at the contact points. Therefore measurements made by adding water to a test section will differ from measurements made by draining water from the section. These two methods usually give a different result than a calculated porosity, determined from the total weight of rocks in a sample (and their associated unit weight) and the total volume of the section. Such discrepancies in measurement are highlighted in DUDGEON (1964), where porosity was measured using these three methods and results varied by up to 10%.

In this series of experiments, porosity was measured by addition of water to a sealed volume containing the test section. The theoretical and measured porosities compare well as illustrated below.

	Material Packing				
	75 mm Spheres		42 mm Spheres		Stone
	Rhombohedral	Cubic	Rhombohedral	Cubic	Random
Porosity-measured	0.26	0.51	0.33	0.52	0.47
Porosity-theoretical	0.24	0.51	0.33	0.49	0.48

Eight oscillatory tests were conducted on each of five samples. The period of oscillation and piston stroke length were varied for each test in each sample. The five test samples are referred to as follows: R75: 75 mm diameter spheres in rhombohedral packing; C75: 75 mm diameter spheres in simple cubic packing; R42: 42 mm diameter spheres in rhombohedral packing; C42: 42 mm diameter spheres in simple cubic packing; S: 100 mm stone sample.

The stroke lengths and approximate periods used for each test are given below.

	Test Number							
	1	2	3	4	5	6	7	8
Period (sec)	12	9	5	8	10	3	6	8
Stroke (cm)	10	10	5	5	5	2.5	2.5	2.5

Characteristic data pertaining to each of the five samples tested includes the porosity (n), grain diameter (D) and steady state Forchheimer coefficients (a_s, b_s), determined from linear regression of the steady flow test results. These data are summarized below.

	Series				
	R75	C75	R42	C42	S
Diameter (mm)	75	75	42	42	100
Porosity	0.26	0.51	0.33	0.52	0.47
a_s (sec/m)	0.41	0.16	0.43	0.08	0.06
b_s (sec/m)^2	19.2	3.43	39.6	8.77	4.94

DATA ANALYSIS

In general, the goal of this paper is to provide a general expression for hydraulic gradient in terms of the driving parameters of the flow. This will eliminate the current requirement when modelling wave-structure interaction of using a flow law such as the Forchheimer or Missbach approximation. Utilization of these methods has been shown to yield erratic results (BRUUN, 1985; HALL, 1991, 1992) when used for rapidly varying, oscillating flow such as that which occurs when a wave interacts with a coastal structure. Numerous drawbacks exist when using a Forchheimer type relationship. HALL *et al.* (1992) have discussed the validity of using steady state-derived Forchheimer coefficients in unsteady oscillatory flow. In addition, the impulsive, jetting nature of waves breaking on to a structure creates localised perturbations in the velocity field. This is not correctly represented by the macroscopic approach inherent in the use of the Forchheimer relationship. Wave breaking produces fully turbulent flow at the wave-structure interact, whereas the macroscopic velocity used in the Forchheimer equation may not be fully turbulent. For the case of wave-structure interaction, a significant difference between the velocity distribution at the face of the structure form that of normal steady porous media flow exists.

Therefore, in applying the Forchheimer relationship to the situation of wave-structure interaction, underestimation of the kinetic energy losses may occur resulting in an underestimation of turbulent losses in the media. This would result in overprediction of the maximum phreatic surface elevation and underestimation of the minimum phreatic surface elevation by the numerical model.

Furthermore, the Forchheimer relationship has

not been extensively verified in the fully turbulent flow regime such as that encountered in the breakwater armour layer. This is because the bulk of porous media research undertaken to date has involved investigation of the flow characteristics of small particles at high flow rates or large particles at low flow rates in which a fully turbulent regime is not reached. DUDGEON (1984) suggested that the non-linear coefficient should be a function of the flow rate. An increase in this parameter at higher flow rates would result in additional turbulent losses.

The experimental results of DUDGEON (1964, 1984) suggest that, in a given medium, the Forchheimer coefficients, a and b, continuously change as the velocity of the flow is increased.

The variation of the Forchheimer a, b coefficients and the inertial coefficient C with characteristics of the driving force has been discussed in HALL *et al.* (1993). A wide variation in the calculated values of a, b and C based on either steady flow or unsteady flow assumptions was found to occur for each media tested. It is therefore desirable to eliminate the need of estimating these coefficients. For this reason, it is desirable to formulate the gradient in terms of the predominant driving characteristics, which for a cyclic unsteady flow through a porous media are the (i) fluid, characterized by ρ, μ; (ii) motion of the fluid, characterized by A, T; (iii) dimension of the material, D; (iv) porosity of the medium, n; and (v) time, t, where ρ = fluid density; μ = fluid viscosity; A = amplitude of water particle oscillation; and T = period of water particle oscillation.

Following dimensional analysis the following generalized statement can be produced

$$a = fxn(\rho, \mu, A, T, n, D, t) \qquad (2)$$

where a = a property of the system which can be written in a dimensionless form as

$$Y_a = \phi_a\left(\frac{\rho D^2}{\mu T}, n, \frac{A}{D}, \frac{t}{T}\right) \qquad (3)$$

where Y_a is a dimensionless form of the property "a" and ϕ_a is a function related specifically to Y_a. The four dimensionless variables are:

$$X_1 = \frac{\rho D^2}{\mu T} \qquad X_2 = n \qquad X_3 = \frac{A}{D} \qquad X_4 = \frac{t}{T}.$$

Each of the above variables reflects the influence of one particular parameter on the system. The variable X_1 reflects the influence of viscosity and is a Reynolds number, R_n, which results from temporal inertia of the system. X_2 is the porosity which is taken to represent the permeability of the system. Effects of particle shape, orientation and surface roughness are therefore considered to be represented by the porosity function. X_3 reflects the influence of stroke amplitude or corresponding water particle amplitude and X_4 is the dimensionless time, required to describe non-stationary systems.

If the quantity a is to be the pressure gradient, I = dH/dx, then the functional relation is

$$Y_1 = \frac{T^2}{\rho D} I = \phi_1(X_1, X_2, X_3, X_4). \qquad (4)$$

Expressing (4) in terms of the hydraulic gradient, $i = I/\rho g$, then

$$i = \frac{D}{gT^2}\phi_1(X_1, X_2, X_3, X_4). \qquad (5)$$

Equation (5) can be expressed in this form as

$$\frac{i}{F_r} = \frac{1}{S_D^2}\phi_1(X_1, X_2, X_3, X_4)$$

where S_D is the Strouhal number based on the grain diameter as the length term, defined as

$$S_D = \frac{q_o T}{D} \qquad (7)$$

and F_r is a Froude Number equal to $\frac{q_o^2}{gD}$ where q_o = bulk flow velocity.

The fact that i/F_r is proportional to $1/S_D^2$ indicates that a slope of -2 should occur if the friction factor is plotted against the Strouhal number, ignoring the effects of the dimensionless variables.

The form of the function ϕ_a is determined from experiments by varying each of the dimensionless variables separately, measuring the results and plotting Y_a against each of the dimensionless variables.

The hydraulic gradient will be expressed in terms of a stationary term, i_o, and a time dependent component i_t. The stationary component will therefore be a function of the first three dimensionless variables, *i.e.*

$$\frac{gT^2}{D} i_o = \phi_o\left(\frac{\rho D^2}{\mu T}, n, \frac{A}{D}\right) \qquad (8)$$

From the experimental measurements, the quantity i_o will be defined as the maximum value of

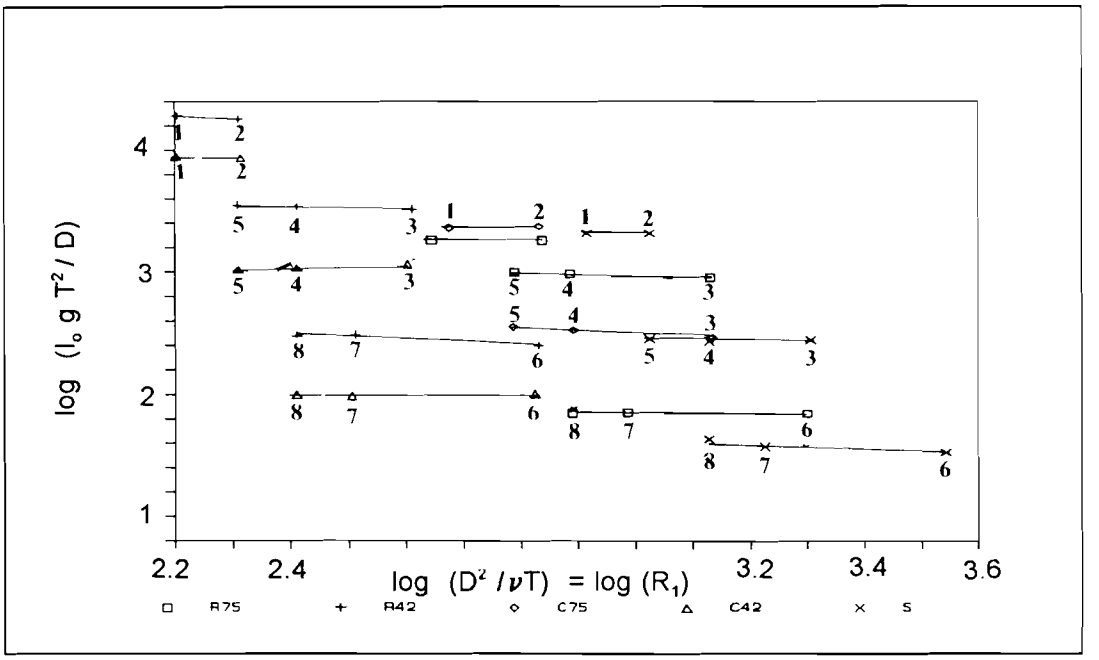

Figure 3. $\frac{i_o g T^2}{D}$ versus R_1.

the gradient record, i_{max}, which occurs over one cycle (one wave length).

To investigate the influence of X_1 on the resistance, the logarithmic plot of $i_o gT^2/D$ against X_1 is shown in Figure 3. No clear trends are evident but some conclusions can be drawn: For a given material, porosity and stroke length, the dimensionless hydraulic gradient is independent of the Reynolds number, R_1. This may be seen by comparing those tests having constant stroke length and varying period (*i.e.* tests 1, 2; tests 3, 4, 5; tests 6, 7, 8). Lines connecting those data points are all horizontal (Figure 3). The differing horizontal and vertical positions of those groups are the result of varying grain size, porosity and stroke length. It may therefore be concluded that the resistance is not affected by the viscosity in the range of flow rates tested. This is not surprising since all tests were conducted far above the laminar regime where the viscosity has the highest influence on the resistance of the medium.

In order to see the influence of the second dimensionless variable, porosity, the natural logarithm of the dimensionless hydraulic gradient, Y_1, is plotted against the porosity in Figure 4. The effect of porosity must be determined by comparing data points where the porosity alone is varied. This is seen by comparing points for a given test number (corresponding to a given period and stroke length) for the same material (D) with different packings. Therefore materials R75 and C75 may be compared, as can R42 and C42. Unfortunately the stone section (S) was only tested with one porosity and cannot be compared to any other points. Lines connecting similar tests are shown on the figure. A correlation can be seen in that all lines have similar slopes of about −5 to −5.5. The varying intercepts are a function of the differing A/D ratios. The general form of the relation can be expressed as

$$\ln\left(\frac{i_o g T^2}{D}\right) = \overline{\alpha_1} + \beta_1 n \qquad (9)$$

or

$$\frac{i_o g T^2}{D} = e^{\overline{\alpha_1} + \beta_1 n} = \alpha_1 e^{\beta_1 n} \qquad (10)$$

where the slope, β_1, is approximately −5 to −5.5 and the intercept, $\alpha_1 = \exp(\overline{\alpha_1})$, varies with grain size and stroke length. This variation is illustrated in Figure 5, which is a plot of the intercept, α_1,

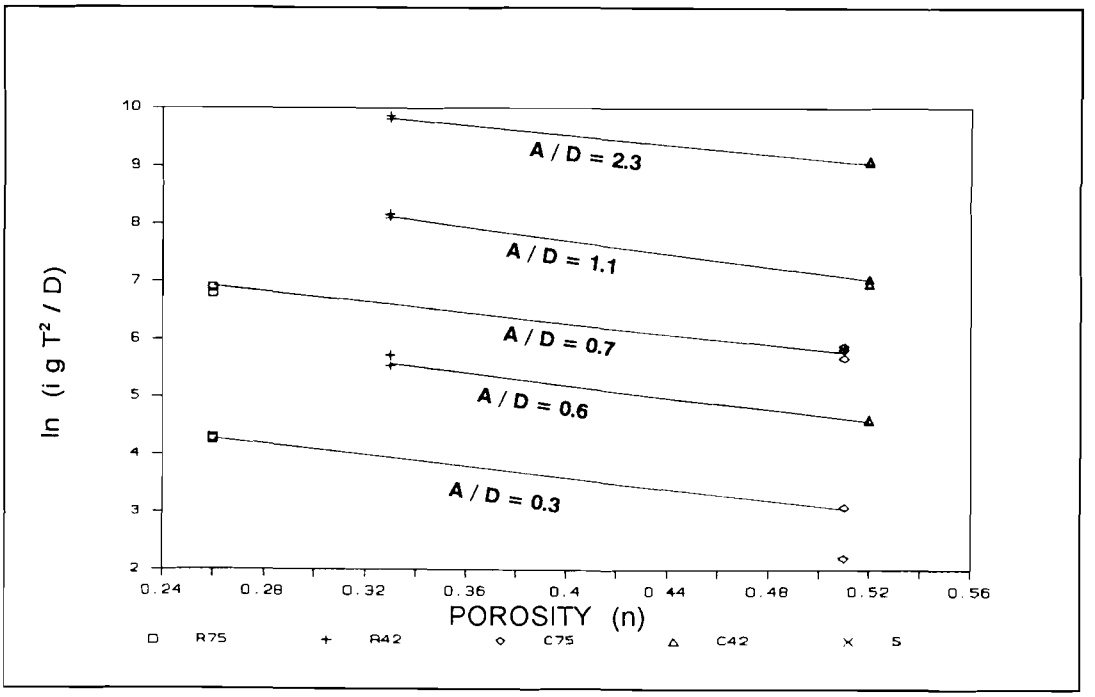

Figure 4. Influence of porosity on energy gradient.

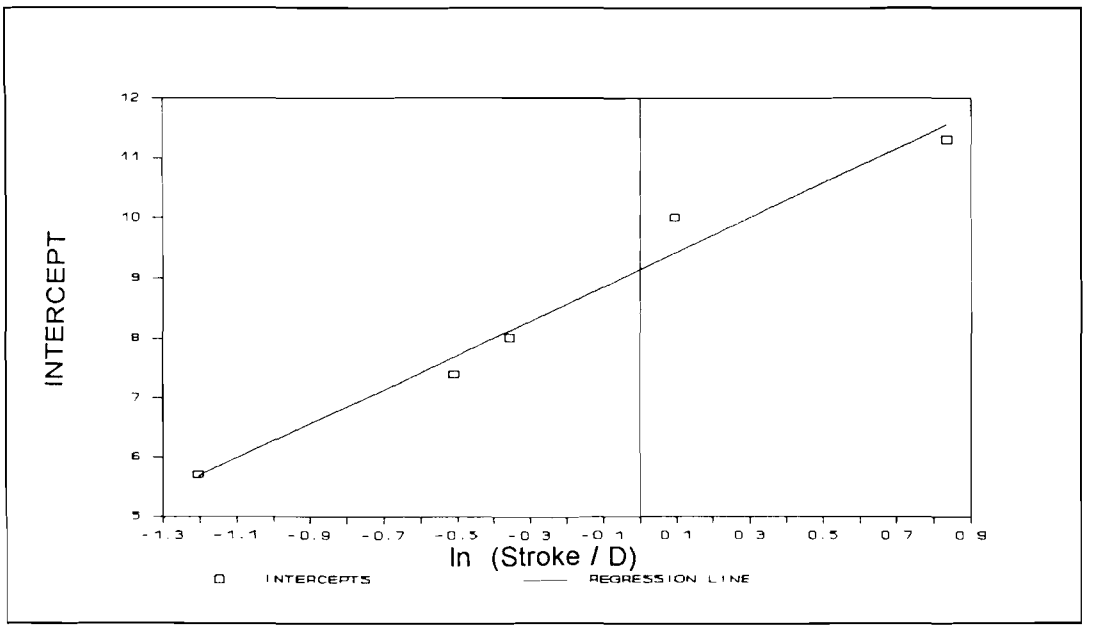

Figure 5. α versus ln(A/D).

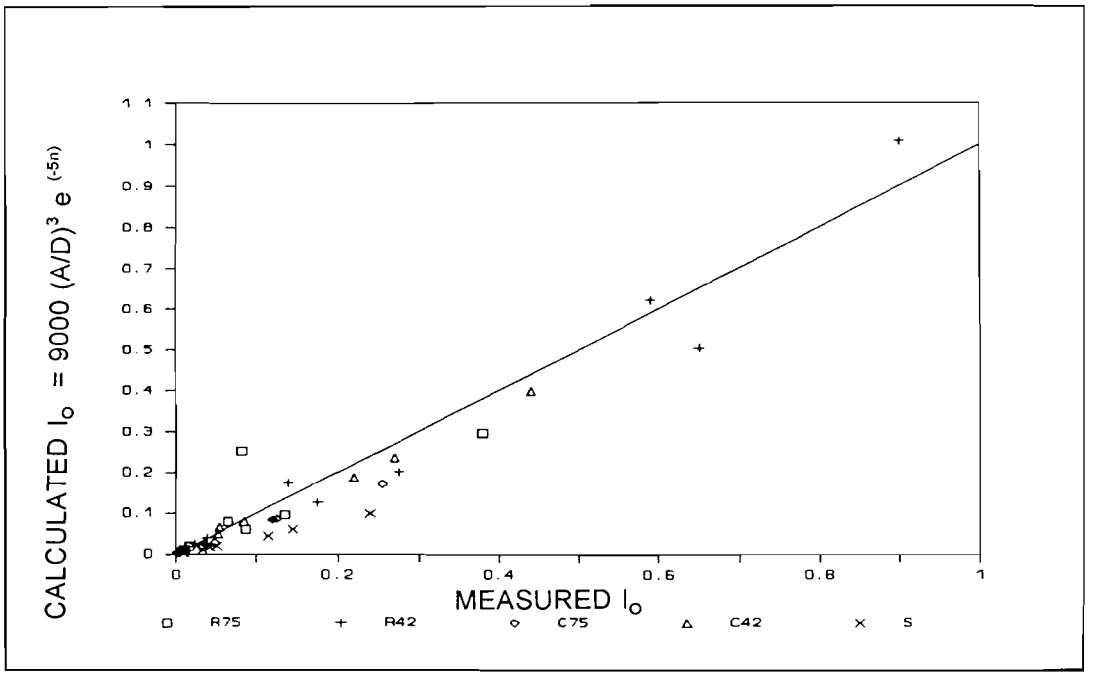

Figure 6. Comparison of calculated and measured i_{max} using (12).

against the natural logarithm of the dimensionless stroke length. The regression equation is

$$\overline{\alpha_1} = 9 + 3 \ln\left(\frac{A}{D}\right) \quad (11)$$

with a correlation coefficient of $r^2 = 0.98$.

Combining equations (9) and (11), the gradient, i_{max}, becomes

$$i_{max} = i_o \approx \frac{D}{gT^2}\left(\frac{A}{D}\right)^3 e^{(9 - 5n)}. \quad (12)$$

A comparison between the maximum measured gradient and the maximum gradient calculated with (12) is presented on Figure 6. The comparison is reasonable. Most of the points tend to fall below the line, indicating that equation (12) tends to underpredict the value of i_{max}. The sum of the squares of the errors is 0.10. From equation (12) the function relating the gradient to the stroke length arose indirectly from consideration of the porosity relation only. To test this relation the dimensionless stroke length will be examined directly.

The logarithm of the dimensionless gradient is plotted against the logarithm of A/D in Figure 7. The trend is seen to be linear with slope of approximately 3 for all test series. This is in accordance with the exponent of 3 found in equation (12). The general equation for this relation is

$$i_o \frac{gT^2}{D} = \alpha_2 \left(\frac{A}{D}\right)^\beta \quad (13)$$

but in this case the intercept is seen to vary with both the porosity, n, and the dimensionless grain size $D^* = \sqrt[3]{\frac{g}{\nu^2}} \cdot D$.

The relations expressed here are limited by the small number of data points and are intended only to give a very general description of the phenomenon. More tests must be conducted before any reliable estimates (not only the values of the coefficients but also for the form of the functions themselves) can be determined. For the spheres tested the intercept, $\log(\alpha_2)$, decreases with increasing porosity (for a given D), and also decreases with decreasing D. From the results of a regression analysis, it was found that

$$\log(\alpha_2) = 3.6 + 4.3 \cdot 10^{-1} \cdot D^* - 2.4n \quad (14)$$

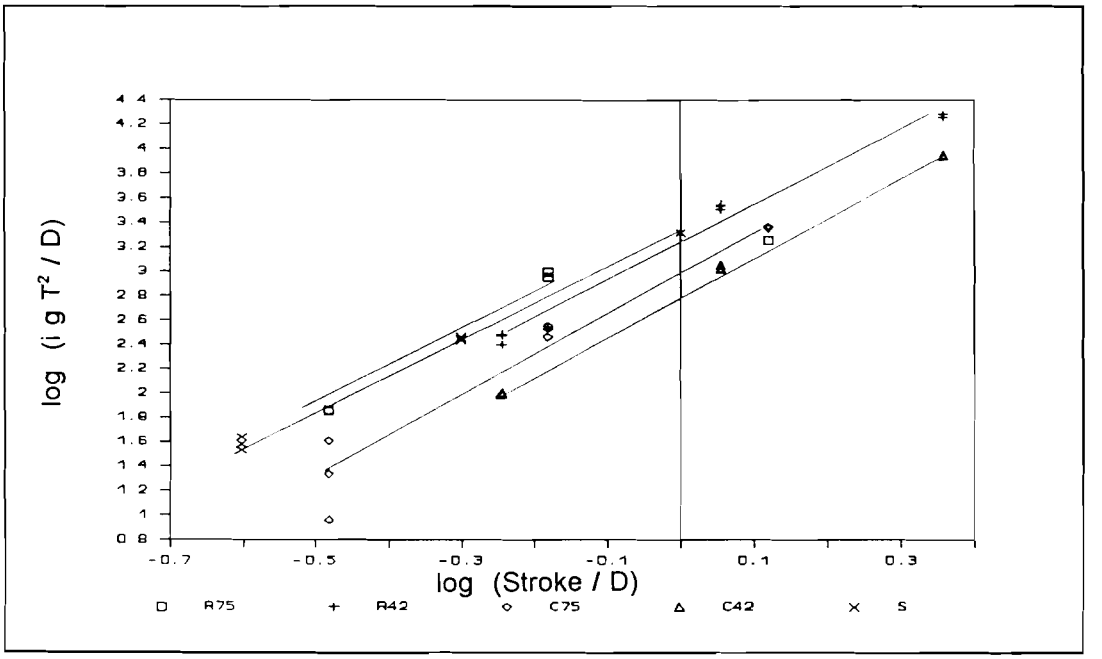

Figure 7. Influence of stroke length on resistance.

The triangles plotted on Figure 8 are computed using (14). The combination of equations (13) and (14) leads to another general form of the equation for the (maximum) hydraulic gradient as

$$i_{max} = i_o \approx \frac{D}{gT^2}\cdot\left(\frac{A}{D}\right)^{n} e^{5.5n} \cdot \exp(8.3 + 9.9\cdot 10^{4}\cdot D^*). \quad (15)$$

This relation differs from the former expression for i_{max} (12), in that (15) involves also a separate term, D*, which comes from the regression analysis and not from the dimensional analysis. This term was introduced to correct the underpredictions of i_o from equation (12). The functions of (A/D) and n, however, are identical.

A comparison of measured values and calculated values for i_{max} (using 15) is presented on Figure 9. Most points fall uniformly about the line of equality. This suggests that the inclusion of the D* term in equation (15) corrects the underpredictions of the gradient in equation (12). The sum of the squares of the errors using equation (15) is 0.11, comparable to that for equation (12).

Non-Stationary Component

The last dimensionless variable, X_4, reflects the time-varying component of the hydraulic gradient. This function will not be a pure sinusoidal curve, partly because the generated pressure gradient was not purely sinusoidal. The proper form of the function can be determined using curve fitting techniques such as Fourier analysis but this task will not contribute significantly to the relationship. For the present it is suffice to say that, for oscillatory flow, the hydraulic gradient can be expressed by

$$i \approx \alpha\frac{D}{gT^2}\left(\frac{A}{D}\right)^{n} e^{5.5n}\cdot\phi_i(t/T) \quad (16)$$

where the coefficient α is, for the values of D tested,

$$\alpha \approx \exp(8.3 + 9.9\cdot 10^{4}\cdot D^*) \quad (17)$$

and $\phi_i(t/T)$ is the time varying function of the driving force.

CONCLUSIONS

The form of the flow law governing oscillatory unsteady flow through porous media was exam-

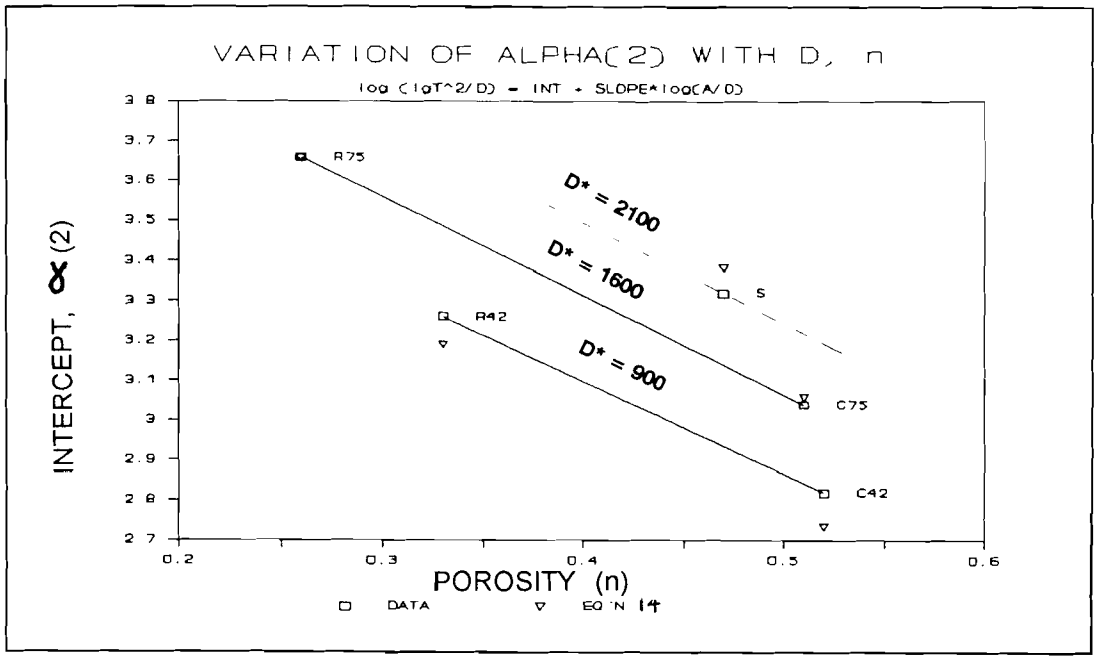

Figure 8. Variation of α_2 with D and n.

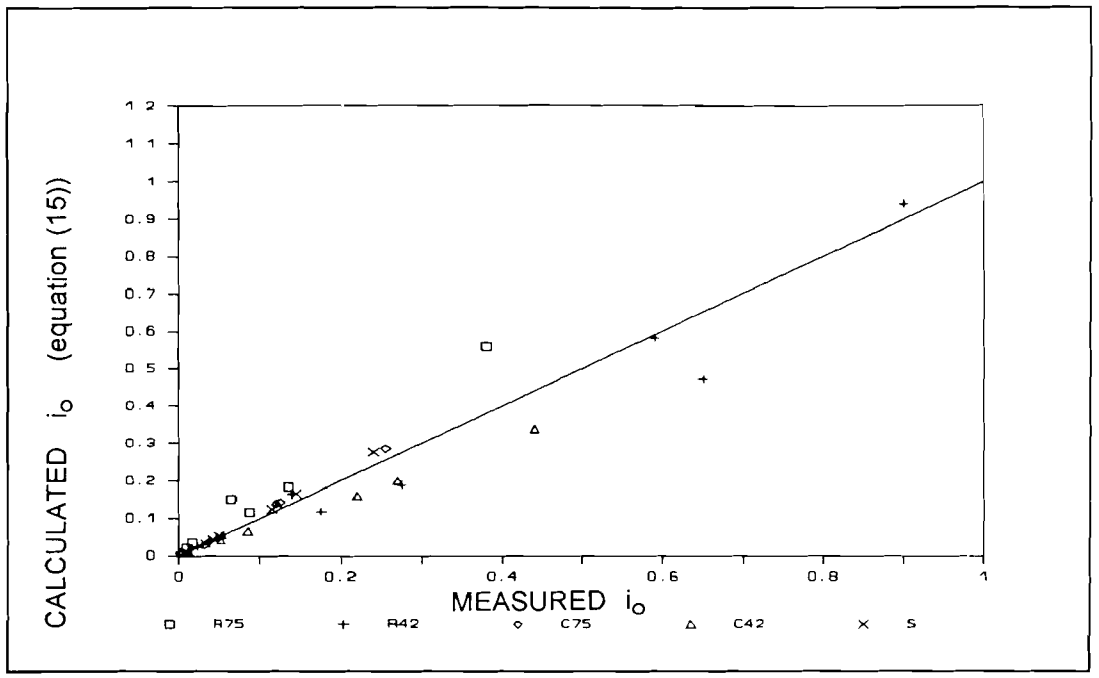

Figure 9. Comparison of measured and calculated i_{max} using (15).

ined and a formulation of the unsteady hydraulic gradient was developed in terms of the parameters describing the medium and those driving the flow.

The stationary component of the hydraulic gradient, i_o, was found to be a function of the inertial Reynolds number, R_I, the porosity, n, the dimensionless water particle motion A/D and a dimensionless grain size term. For flow beyond the laminar regime, i_o is independent of R_I. The variation of i_o with porosity was shown to be exponential. The variation of i_o with A/D was described by a power function with an exponent of 3. The complete expression for hydraulic gradient was determined to

$$i \approx \alpha \frac{D}{gT^2}\left(\frac{A}{D}\right)^{\beta} e^{\gamma n} \cdot \phi_i\left(\frac{t}{T}\right)$$

where $\alpha \approx \exp(8.3 + 9.9 \cdot 10^{-1} \cdot D^*)$, $\beta \approx 3$, and $\gamma \approx -5.5$ for the media and flow conditions tested. D^* is a dimensionless grain size defined as $D^* = \sqrt[3]{\frac{g}{\nu^2}} \cdot D$.

The form of the function $\phi_i(t/T)$ can be determined from curve fitting techniques.

LITERATURE CITED

BRUUN, P., 1985. The design and construction of mounds for breakwaters and coastal protection. Amsterdam: Elsevier.

DUDGEON, C.R., 1964. Flow of Water Through Coarse Granular Materials. M. Eng. Thesis, Sydney, Australia: University of New South Wales, 109p.

DUDGEON, C.R., 1968. Relationship between porosity and permeability of coarse granular materials, Proceedings 3rd Australian Conference on Hydraulics and Fluid Mechanics (IEA, Sydney), pp. 76–80.

DUDGEON, C.R., 1984. Non-darcy Flow of Groundwater. Ph.D. Thesis, Sydney, Asutralia: University of New South Wales.

DYBBS, A. and EDWARDS, R.V., 1982. A new look at porous media fluid mechanics—Darcy to turbulent. *In:* BEAR, J. and CORAPCIOGLU, M.Y. (eds.), *Fundamentals of Transport Phenomenon in Porous Media*, New York: NATO ASI, Series E: Applied Sciences, No. 82, pp. 199–256.

Hall, K.R., 1987. A Study of the Stability of Rubblemound Breakwaters. Ph.D. Thesis, Sydney, Australia: University of New South Wales.

HALL, K.R., 1991. Trends in phreatic surface motion in rubblemound breakwaters. *ASCE Journal of Waterway, Port, Coastal and Ocean Engineering*, 117(2), 179–184.

HALL, K.R., 1992. Prediction of free surface position and fluid pressure in rubblemound breakwater. *Transactions of the College of Civil Engineers, Institution of Engineers, Australia*, CE 34, No. 1, April 1992, pp. 9–19.

HALL, K.R. and SMITH, G.M., 1992. Comparison of measured and predicted Forchheimer coefficients in oscillatory unsteady flow, submitted to ASCE Journal of Waterway, Port, Coastal and Ocean Engineering, Dec., 1992.

HALL, K.R.; SMITH, G.M., and TURCKE, D.J., 1992. Comparison of oscillatory and stationary flow through porous media, submitted to Coastal Engineering Journal, Dec., 1992.

HALL, K.R.; SMITH, G.M., and TURCKE, D.J., 1993. Variation in porous media flow characteristics with oscillatory flow characteristics, submitted to ASCE Journal of Waterway, Port, Coastal and Ocean Engineering, Jan., 1993.

HALL, K.R.; SMITH, G.M., and TURCKE, D.J., 1992. Comparison of oscillatory and stationary flow through porous media, submitted to Coastal Engineering Journal, Dec., 1992.

ROSE, H.E. and RIZK, A.M.A., 1948. Further researches in fluid flow through beds of granular material. *Institution of Mechanical Engineers Proceedings*, 160, 493–148.

WRIGHT, D.E., 1968. Non-linear flow through granular media. *Journal Hydraulics Division* (ASCE) 94, No. HY4, pp. 851–872.